(Received 5 December 2025, Accepted 9 February 2026, Scheduled 18 March 2026)

Millimeter Wave Wideband Patch Antenna with DGS Slots and Truncated Corners for 5G Applications

Ruchika Singh[1,*] and Mukesh Arora[2]

[1] ECE Department, Rajasthan Technical University, Kota, Rajasthan, India
[2] ECE Department, SKIT, Jaipur 302017, India

ABSTRACT: This paper presents the design, simulation, fabrication, and experimental validation of a compact millimeter-wave microstrip patch antenna intended for fifth generation (5G) wireless applications. The proposed antenna employs a coplanar waveguide (CPW) feed, a defected ground structure (DGS), and truncated patch corners to enhance impedance bandwidth and radiation characteristics while maintaining a compact footprint. The antenna is designed on a Rogers RT/Duroid 5880 substrate ($\varepsilon_r = 2.2$, $\tan\delta = 0.0009$, thickness $= 0.502$ mm) and operates in the Ka-band with a center frequency of 30 GHz. Measured results demonstrate an impedance bandwidth from 29 to 34 GHz and a peak realized gain of 7 dBi, showing good agreement with simulated predictions. These results indicate that the proposed antenna is a suitable candidate for compact 5G millimeter-wave communication systems.

1. INTRODUCTION

Improvements in areas such as antenna size, bandwidth, gain, power loss, traffic demand, and data rate are needed due to the increasing needs of today's wireless and radio communication systems. Consequently, several designs have been developed to strike a balance between these conflicting needs for high data rate, low cost, low power consumption, small size, and high bandwidth antennas [1–9]. Since the speed of the impending Fifth Generation (5G) will be five times that of the current Fourth Generation (4G), this is a reasonable assumption to make. The data rate, bandwidth, and storage capacity will all be quite high. The upcoming 5G technology may have its roots in millimeter wave radio frequency. Millimeter waves can meet the demands of the next generation since they use the untapped spectrum between 3 and 300 gigahertz. The frequency range for 5G use is 20–90 GHz [2]. Because of their limited beamwidth, they are useful for cellular applications while being highly directed and sensitive to obstructions [4].

Although there is a wide variety of substrates to choose from, the ideal one for millimeter waves is Rogers substrate since all other substrates have dielectric constants that are lower than 10 GHz [1]. It is best suited for ultra-high frequency (UHF). Low water absorption, low electric loss, and low moisture absorption are all features of a Rogers substrate [10, 11]. Metal should be used on both sides. The top layer forms the radiating patch and feeding structure, while the bottom layer acts as the ground plane. Because of the necessity for a gain of 12 dB in mobile communication, M-line feeding is employed. This paper's focus is on the Ka-band (27–40 GHz) and its associated 30 GHz centre frequency [11]. The planar inverted F-shape antenna (PIFA) reported in [3] operates at 28 GHz and 38 GHz and demonstrates improved bandwidth performance compared with conventional single-band mmWave antenna designs. Using transformer coupling, the authors of [5] achieve a gain of 6.02 dBi and an efficiency of 83.03% at 30 GHz. The suggested antenna has good bandwidth, radiation efficiency, and gain, and can operate at 30 GHz.

These exponential developments of wireless devices over the years have led to major advancements in the development of cutting-edge standards for communication networks. High-throughput and high-data-rate requirements are met by 4G LTE's effective combination of many commercial services within the capacity of already-deployed networks, and the technology also provides lightning-fast access to end users. However, bandwidth constraints have emerged because of this extensive upgrade, which further limits necessary developments while using up precious spectrum of just around 3 GHz.

It is expected that the high capacity and throughput requirements of future 5G networks may be addressed by the available spectrum in the millimeter-wave (MMW) range [1–3]. Problems with signal attenuation, route loss, and air absorption are most pressing in the mmWave range. To account for the channel characteristics in the radio wave propagation medium, it is also necessary to undertake a comprehensive radio frequency (RF) link budget analysis [14]. Capacity without needing more spectrum or transmission power by using several antennas at once with the use of multiple-input multiple-output (MIMO) designs, faster data rates, and multi-Gbps throughput may be provided for dependable communications [5, 6]. Strong bandwidth to support multiple system services at once, strong gain to overcome absorptions, and structural simplicity for MIMO system integration are the top priorities for the 5G MIMO antenna [9]. Additionally, the planned antenna shape must be small so that it may be integrated into portable cellular devices.

* Corresponding author: Ruchika Singh (rsruchi009@gmail.com).

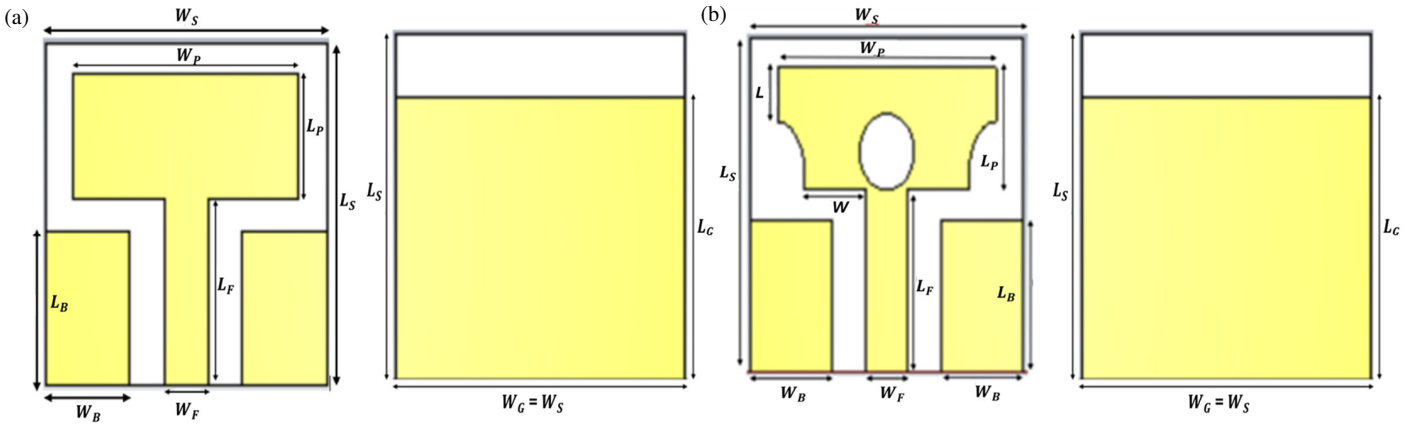

FIGURE 1. (a) Initial design front & back of CPW feed antenna with DGS, and (b) front & back of CPW feed antenna with DGS, slots and truncated corners.

Several methods [10–13] have been tried to lessen the mutual coupling between the various parts of a MIMO antenna.

Smaller antenna size at mmWave frequencies is a benefit since it allows for the compact placement of many components with less mutual interaction. The patch antenna's flat, small, and resilient shape has made it a hot topic in the realm of wireless devices and integrated circuits. Lower gain and bandwidth are the primary issues; however, they may be greatly increased by using a variety of methods. Specifically, a defective ground structure (DGS) was devised by purposefully creating a 'fault' in the ground's planar shape to boost antenna performance [14].

These flaws cause generated perturbations that destroy ground plane homogeneity and surface current continuity [15–18]. To efficiently couple with the feed line, symmetrical DGS structures are built immediately beneath or on either side of the microstrip line [18–20]. DGS also modifies the ground's shield current distribution in accordance with the defect's form and size, allowing for regulated excitation and electromagnetic propagation through the substrate and, by extension, modifying the transmission line's capacitive and inductive responses [19, 21, 22].

That is, DGS may boost the band notching capabilities by increasing the effective capacitance and inductance [23], leading to various resonant frequencies and so producing a multiband antenna [24]. By carefully choosing the geometry of the faults and placing them in strategic spots, the constructed antenna may be tuned to the required resonant frequency.

2. THE ANTENNA DESIGN GEOMETRY

The proposed antenna geometry consists of a rectangular radiating patch excited through a coplanar waveguide (CPW) feed and backed by a defected ground plane, as shown in Fig. 1(a). Rogers RT/Duroid 5880 substrate with a relative permittivity of 2.2, loss tangent of 0.0009, and thickness of 0.502 mm is selected to minimize dielectric losses at millimetre-wave frequencies. The substrate dimensions are 10 mm × 11 mm, ensuring compactness suitable for portable 5G devices.

Initially, a conventional rectangular patch resonating at approximately 30 GHz is designed. To suppress unwanted resonances and improve impedance matching, an elliptical slot is introduced at the centre of the patch, while the lower corners of the patch are truncated in a quarter-ellipse shape (Fig. 1(b)). These modifications alter the surface current distribution and effectively broaden the operating bandwidth. The defected ground structure is realized by removing a portion of the ground plane beneath the CPW feed, further contributing to bandwidth enhancement.

TABLE 1. Dimensions of proposed antenna for 5G.

Parameters	Description	Value (mm)
L_S	Length of Substrate	11
W_S	Width of Substrate	10
L_P	Length of Patch	8
W_P	Width of Patch	4
L_G	Length of Ground	9
W_G	Width of Ground	10
L_F	Length of Feed Line	6
W_F	Width of Feed Line	1.5
L	Length of Slotted Patch	2.25
W	Width of Slotted Patch	2.25
L_B	Length of CPW	5
W_B	Width of CPW	3

All design parameters shown in Table 1 are optimized using Computer Simulation Technology (CST) Microwave Studio. The final antenna dimensions are selected to achieve a wide impedance bandwidth, stable radiation patterns, and adequate gain across the operating frequency range.

3. RESULTS AND COMPARISON

3.1. Simulation

The simulated reflection coefficient indicates strong impedance matching around the center frequency of 30 GHz, with a minimum $|S_{11}|$ below −50 dB. The −10 dB impedance bandwidth spans approximately 27.5–32.5 GHz, covering a significant portion of the Ka-band. Fig. 3(a) shows the simulated return loss. Fig. 3(c) shows that the corresponding voltage standing

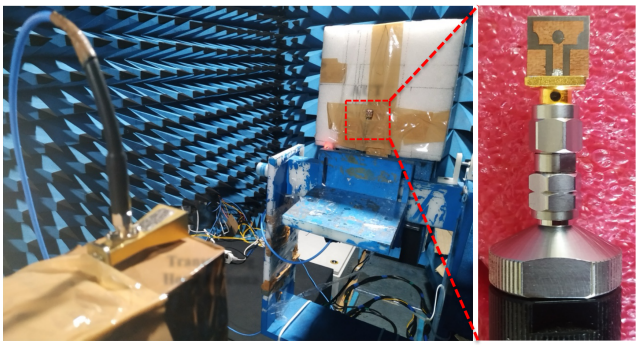

FIGURE 2. Experimental setup inside an anechoic chamber to measure the radiation and gain of the proposed antenna.

TABLE 2. Comparison of the proposed wideband antenna with similar works reported earlier.

References	[25]	[26]	[27]	[28]	[29]	[30]	[31]	[32]	[33]	[34]	Proposed work
Freq.(GHz)	3.5	5.8	3.6	2.46	4.9	2.3	5.5	25	1.96-19.59	2.44,10.16	29-34
BW	Narrow	Narrow	Narrow	Narrow	Narrow		Narrow	Narrow	Ultra wideband	wideband	Wideband
Method	Coupled line resonator	Polarization conversion	Slot combined CSRR	1D EBG+SRR	EBG+SRR	Fractal DGS	Absorber	CSRR	DGS with rectangular slots	DGS with ring shape	DGS with truncated corners
Gain(dBi)	6.25	<5	3.59	2.57	<5	5	7.74	NA	4.5	6.28	7
Efficiency(%)	87	60	NA	82	75	96	68.03	NA	90	90	77
FTBR(dB)	16	13	20	9.3	10	9	15.2	NA	NA		10.3

wave ratio (VSWR) remains close to unity at the resonant frequency, confirming efficient power transfer.

The simulated realized gain varies across the operating band, with a peak value of approximately 8 dBi observed at higher frequencies and a gain of about 3.5 dBi at 30 GHz. Fig. 3(b) shows the simulated gain. This variation is attributed to frequency-dependent radiation efficiency and current distribution. Simulated radiation patterns in both the E-plane and H-plane, in Figs. 4(a) and (b), exhibit stable broadside radiation with good co-polarization to cross-polarization isolation, indicating satisfactory polarization purity.

3.2. Measurements

Figure 2 shows the prototype of the antenna, including truncated corners and defected ground slot. The prototype is printed on RT Duroid 5880 with dielectric constant (ε_r) of 2.2, loss tangent ($\tan\delta$) of 0.0009, and height (h) of 0.502 mm using a standard printed circuit board (PCB) laminate process. The prototype is evaluated using both simulation and measurement techniques to validate its performance in real-world scenarios. A vector network analyzer (VNA) is utilized to measure the S-parameters of the antenna system, including return loss and VSWR of the antenna. The model of the VNA is the PNA N5224B, whose operating frequency range is from 10 MHz to 43.5 GHz. The gain and radiation patterns of the antenna were measured inside an anechoic chamber using the setup as shown in Fig. 2. A broadband double-ridged horn antenna (operating range 18–40 GHz) was used as a transmitter (Tx); the distance between the Tx horn and the device under test (DUT) was kept at 90 cm to ensure radiation measurement in the far-field.

The measured 10 dB impedance bandwidth (BW) of the antenna is found from 29 to 34 GHz with the maximum matching of better than 38 dB at 30.8 GHz (Fig. 3(a)). The measured VSWR remains close to unity over 30.5–31.3 GHz, shown in Fig. 3(c). The gain and 2D radiation pattern of the antenna were measured inside an anechoic chamber, and the results were found in good accordance with the simulated response. The measured peak realized gains are 7 dBi at 29.3 GHz and 3 dBi gain at 30 GHz.

The measured gain is shown in Fig. 3(b). The 2D patterns of the antenna were measured in two principal planes, E and H, shown in Figs. 4(c) and (d). In both planes, the measured patterns follow a similar correlation to that of the simulated ones. The antenna exhibits a good cross-polarization (X-pol) in both planes with 77% efficiency.

The slight discrepancy between simulated and measured values is attributed to fabrication tolerances, connector losses, and material parameter variations at millimeter-wave frequencies. Nevertheless, the overall measured trends closely follow the simulated predictions. The comparison of the parameters of

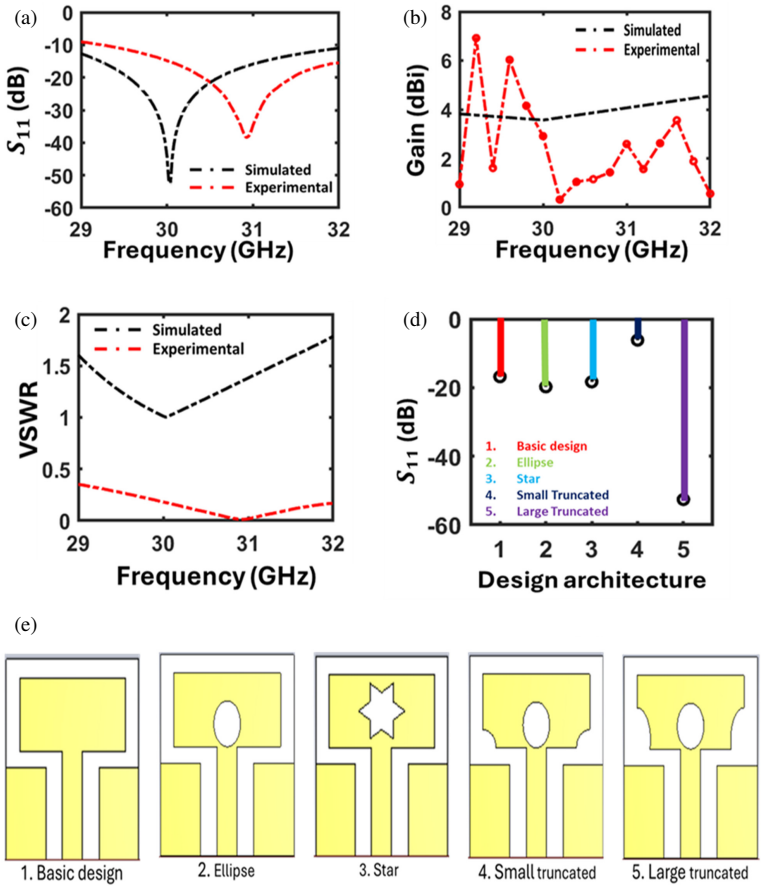

FIGURE 3. Comparison between simulated and measured results, (a) return loss, (b) gain, (c) VSWR, (d) comparison of return loss between different design architectures, (e) different design architectures.

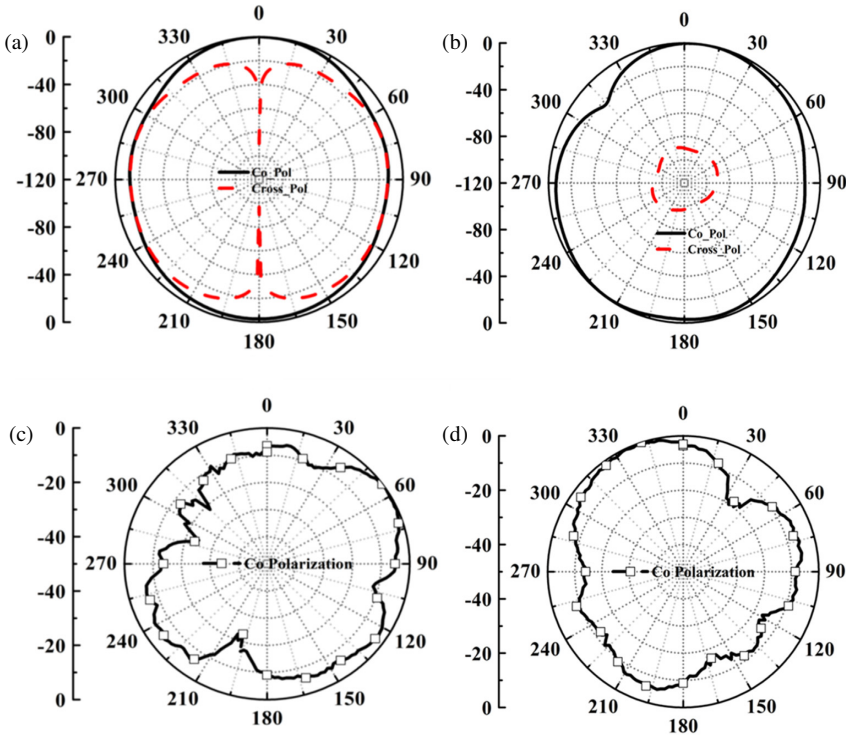

FIGURE 4. Radiation patterns of the antenna at 30 GHz. (a) Simulated E-plane. (b) Simulated H-plane. (c) Measured E-plane. (d) Measured H-plane.

the proposed design with previous reports is demonstrated in Table 2 [25–34].

3.3. Compared Results

The compared results of simulation and measurement are shown below. Fig. 3(a) shows the comparison between return losses. Fig. 3(b) shows the gain comparison. Fig. 3(c) shows the VSWR comparison. Fig. 3(d) shows the compared return loss between different design architectures, and all the designs are shown in Fig. 3(e).

4. CONCLUSION

A high-performance DGS-based MMW antenna has been designed, simulated, fabricated, and measured. A bandwidth of 3.64 GHz with a centre frequency of 30 GHz has been reported for 5G applications. The design methodology and performance analysis of the proposed MMW antenna have been discussed. To design an efficient antenna with high bandwidth, the suggested antenna geometry comprises a CPW-fed radiating patch and a partial ground plane. Measured results show an impedance bandwidth of 29 to 34 GHz and a high-gain profile with a peak gain of 7 dBi at 29.3 GHz, which are in good agreement with the simulated results. These aspects suggest that the proposed MMW antenna is a promising candidate for 5G applications, particularly in cellular infrastructure.

REFERENCES

[1] Outerelo, D. A., A. V. Alejos, M. G. Sanchez, and M. V. Isasa, "Microstrip antenna for 5G broadband communications: Overview of design issues," in *2015 IEEE International Symposium on Antennas and Propagation & USNC/URSI National Radio Science Meeting*, 2443–2444, Vancouver, BC, Canada, 2015.

[2] Al-Falahy, N. and O. Y. K. Alani, "Design considerations of ultra dense 5G network in millimetre wave band," in *2017 Ninth International Conference on Ubiquitous and Future Networks (ICUFN)*, 141–146, Milan, Italy, 2017.

[3] Ahmad, W. and W. T. Khan, "Small form factor dual band (28/38 GHz) PIFA antenna for 5G applications," in *2017 IEEE MTT-S International Conference on Microwaves for Intelligent Mobility (ICMIM)*, 21–24, Nagoya, Japan, 2017.

[4] Wu, T.-Y. and T. Chang, "Interference reduction by millimeter wave technology for 5G-based green communications," *IEEE Access*, Vol. 4, 10 228–10 234, 2016.

[5] Roy, P., R. K. Vishwakarma, A. Jain, and R. Singh, "Multiband millimeter wave antenna array for 5G communication," in *2016 International Conference on Emerging Trends in Electrical Electronics & Sustainable Energy Systems (ICETEESES)*, 102–105, Sultanpur, India, 2016.

[6] Chen, X.-P., K. Wu, L. Han, and F. He, "Low-cost high gain planar antenna array for 60-GHz band applications," *IEEE Transactions on Antennas and Propagation*, Vol. 58, No. 6, 2126–2129, Jun. 2010.

[7] Biglarbegian, B., M. Fakharzadeh, D. Busuioc, M.-R. Nezhad-Ahmadi, and S. Safavi-Naeini, "Optimized microstrip antenna arrays for emerging millimeter-wave wireless applications," *IEEE Transactions on Antennas and Propagation*, Vol. 59, No. 5, 1742–1747, May 2011.

[8] Wang, L., Y.-X. Guo, and W.-X. Sheng, "Wideband high-gain 60-GHz LTCC L-probe patch antenna array with a soft surface," *IEEE Transactions on Antennas and Propagation*, Vol. 61, No. 4, 1802–1809, Apr. 2013.

[9] Li, M. and K.-M. Luk, "Low-cost wideband microstrip antenna array for 60-GHz applications," *IEEE Transactions on Antennas and Propagation*, Vol. 62, No. 6, 3012–3018, Jun. 2014.

[10] Pozar, D. M. and D. H. Schaubert, *Microstrip Antennas: The Analysis and Design of Microstrip Antennas and Arrays*, 1st ed., 448, Wiley-IEEE Press, 1995.

[11] Gupta, R. K., T. Shanmuganantham, and R. Kiruthika, "A staircase hexagonal shaped microstrip patch antenna for multiband applications," in *2016 International Conference on Control, Instrumentation, Communication and Computational Technologies (ICCICCT)*, 298–303, Kumaracoil, India, 2016.

[12] Kaur, N. and S. Malhotra, "A review on significance of design parameters of microstrip patch antennas," in *2016 5th International Conference on Wireless Networks and Embedded Systems (WECON)*, 1–6, Rajpura, India, 2016.

[13] Saini, J. and S. K. Agarwal, "Design a single band microstrip patch antenna at 60 GHz millimeter wave for 5G application," in *2017 International Conference on Computer, Communications and Electronics (Comptelix)*, 227–230, Jaipur, India, 2017.

[14] Hong, W., K.-H. Baek, and S. Ko, "Millimeter-wave 5G antennas for smartphones: Overview and experimental demonstration," *IEEE Transactions on Antennas and Propagation*, Vol. 65, No. 12, 6250–6261, 2017.

[15] Hashem, Y. A. M. K., O. M. Haraz, and E.-D. M. El-Sayed, "6-Element 28/38 GHz dual-band MIMO PIFA for future 5G cellular systems," in *2016 IEEE International Symposium on Antennas and Propagation (APSURSI)*, 393–394, Fajardo, PR, USA, 2016.

[16] Rappaport, T. S., S. Sun, R. Mayzus, H. Zhao, Y. Azar, K. Wang, G. N. Wong, J. K. Schulz, M. Samimi, and F. Gutierrez, "Millimeter wave mobile communications for 5G cellular: It will work!" *IEEE Access*, Vol. 1, 335–349, 2013.

[17] Rappaport, T. S., J. N. Murdock, and F. Gutierrez, "State of the art in 60-GHz integrated circuits and systems for wireless communications," *Proceedings of the IEEE*, Vol. 99, No. 8, 1390–1436, 2011.

[18] Pi, Z. and F. Khan, "An introduction to millimeter-wave mobile broadband systems," *IEEE Communications Magazine*, Vol. 49, No. 6, 101–107, 2011.

[19] Rahimian, A. and F. Mehran, "RF link budget analysis in urban propagation microcell environment for mobile radio communication systems link planning," in *2011 International Conference on Wireless Communications and Signal Processing (WCSP)*, 1–5, Nanjing, China, Nov. 2011.

[20] Hussain, R., A. T. Alreshaid, S. K. Podilchak, and M. S. Sharawi, "Compact 4G MIMO antenna integrated with a 5G array for current and future mobile handsets," *IET Microwaves, Antennas & Propagation*, Vol. 11, No. 2, 271–279, 2017.

[21] Li, Y., C. Wang, H. Yuan, N. Liu, H. Zhao, and X. Li, "A 5G MIMO antenna manufactured by 3-D printing method," *IEEE Antennas and Wireless Propagation Letters*, Vol. 16, 657–660, 2017.

[22] Wu, D., S. W. Cheung, T. I. Yuk, and X. Sun, "A planar MIMO antenna for mobile phones," in *PIERS Proceedings*, 1150–1152, Taipei, Taiwan, Mar. 2013.

[23] Zhao, Q. and J. Li, "Rain attenuation in millimeter wave ranges," in *2006 7th International Symposium on Antennas, Propagation & EM Theory*, 1–4, Guilin, China, 2006.

[24] Ouyang, J., F. Yang, and Z. M. Wang, "Reducing mutual coupling of closely spaced microstrip MIMO antennas for WLAN application," *IEEE Antennas and Wireless Propagation Letters*, Vol. 10, 310–313, 2011.

[25] Vishvaksenan, K. S., K. Mithra, R. Kalaiarasan, and K. S. Raj, "Mutual coupling reduction in microstrip patch antenna arrays using parallel coupled-line resonators," *IEEE Antennas and Wireless Propagation Letters*, Vol. 16, 2146–2149, 2017.

[26] Cheng, Y.-F., X. Ding, W. Shao, and B.-Z. Wang, "Reduction of mutual coupling between patch antennas using a polarization-conversion isolator," *IEEE Antennas and Wireless Propagation Letters*, Vol. 16, 1257–1260, Nov. 2016.

[27] Yang, X. M., X. G. Liu, X. Y. Zhou, and T. J. Cui, "Reduction of mutual coupling between closely packed patch antennas using waveguided metamaterials," *IEEE Antennas and Wireless Propagation Letters*, Vol. 11, 389–391, 2012.

[28] Lee, J.-Y., S.-H. Kim, and J.-H. Jang, "Reduction of mutual coupling in planar multiple antenna by using 1-D EBG and SRR structures," *IEEE Transactions on Antennas and Propagation*, Vol. 63, No. 9, 4194–4198, 2015.

[29] Liu, Y., X. Yang, Y. Jia, and Y. J. Guo, "A low correlation and mutual coupling MIMO antenna," *IEEE Access*, Vol. 7, 127 384–127 392, 2019.

[30] Wei, K., J.-Y. Li, L. Wang, Z.-J. Xing, and R. Xu, "Mutual coupling reduction by novel fractal defected ground structure bandgap filter," *IEEE Transactions on Antennas and Propagation*, Vol. 64, No. 10, 4328–4335, Oct. 2016.

[31] Garg, P. and P. Jain, "Isolation improvement of MIMO antenna using a novel flower shaped metamaterial absorber at 5.5 GHz WiMAX band," *IEEE Transactions on Circuits and Systems II: Express Briefs*, Vol. 67, No. 4, 675–679, Apr. 2020.

[32] Selvaraju, R., M. H. Jamaluddin, M. R. Kamarudin, J. Nasir, and M. H. Dahri, "Mutual coupling reduction and pattern error correction in a 5G beamforming linear array using CSRR," *IEEE Access*, Vol. 6, 65 922–65 934, 2018.

[33] Lakshmaiah, Y. V. and B. Roy, "Planar monopole antenna based on surface roughness and stub loaded with notch controlling characteristics," *Transactions on Electrical and Electronic Materials*, Vol. 24, No. 6, 502–510, Aug. 2023.

[34] Lakshmaiah, Y. V. and B. Roy, "A circular monopole antenna for bandwidth enhancement using cylinder slots with triple band notch characteristics," *International Journal of Communication Systems*, Vol. 36, No. 7, e5453, May 2023.